

Measurement of the $B \rightarrow \pi \ell \nu$ Branching Fraction and Determination of $|V_{ub}|$ with Tagged B Mesons

B. Aubert,¹ R. Barate,¹ M. Bona,¹ D. Boutigny,¹ F. Couderc,¹ Y. Karyotakis,¹ J. P. Lees,¹ V. Poireau,¹ V. Tisserand,¹ A. Zghiche,¹ E. Grauges,² A. Palano,³ J. C. Chen,⁴ N. D. Qi,⁴ G. Rong,⁴ P. Wang,⁴ Y. S. Zhu,⁴ G. Eigen,⁵ I. Ofte,⁵ B. Stugu,⁵ G. S. Abrams,⁶ M. Battaglia,⁶ D. N. Brown,⁶ J. Button-Shafer,⁶ R. N. Cahn,⁶ E. Charles,⁶ M. S. Gill,⁶ Y. Groyzman,⁶ R. G. Jacobsen,⁶ J. A. Kadyk,⁶ L. T. Kerth,⁶ Yu. G. Kolomensky,⁶ G. Kukartsev,⁶ G. Lynch,⁶ L. M. Mir,⁶ T. J. Orimoto,⁶ M. Pripstein,⁶ N. A. Roe,⁶ M. T. Ronan,⁶ W. A. Wenzel,⁶ P. del Amo Sanchez,⁷ M. Barrett,⁷ K. E. Ford,⁷ T. J. Harrison,⁷ A. J. Hart,⁷ C. M. Hawkes,⁷ S. E. Morgan,⁷ A. T. Watson,⁷ T. Held,⁸ H. Koch,⁸ B. Lewandowski,⁸ M. Pelizaeus,⁸ K. Peters,⁸ T. Schroeder,⁸ M. Steinke,⁸ J. T. Boyd,⁹ J. P. Burke,⁹ W. N. Cottingham,⁹ D. Walker,⁹ T. Cuhadar-Donszelmann,¹⁰ B. G. Fulsom,¹⁰ C. Hearty,¹⁰ N. S. Knecht,¹⁰ T. S. Mattison,¹⁰ J. A. McKenna,¹⁰ A. Khan,¹¹ P. Kyberd,¹¹ M. Saleem,¹¹ D. J. Sherwood,¹¹ L. Teodorescu,¹¹ V. E. Blinov,¹² A. D. Bukin,¹² V. P. Druzhinin,¹² V. B. Golubev,¹² A. P. Onuchin,¹² S. I. Serednyakov,¹² Yu. I. Skovpen,¹² E. P. Solodov,¹² K. Yu Todyshev,¹² D. S. Best,¹³ M. Bondioli,¹³ M. Bruinsma,¹³ M. Chao,¹³ S. Curry,¹³ I. Eschrich,¹³ D. Kirkby,¹³ A. J. Lankford,¹³ P. Lund,¹³ M. Mandelkern,¹³ R. K. Mommsen,¹³ W. Roethel,¹³ D. P. Stoker,¹³ S. Abachi,¹⁴ C. Buchanan,¹⁴ S. D. Foulkes,¹⁵ J. W. Gary,¹⁵ O. Long,¹⁵ B. C. Shen,¹⁵ K. Wang,¹⁵ L. Zhang,¹⁵ H. K. Hadavand,¹⁶ E. J. Hill,¹⁶ H. P. Paar,¹⁶ S. Rahatlou,¹⁶ V. Sharma,¹⁶ J. W. Berryhill,¹⁷ C. Campagnari,¹⁷ A. Cunha,¹⁷ B. Dahmes,¹⁷ T. M. Hong,¹⁷ D. Kovalskiy,¹⁷ J. D. Richman,¹⁷ T. W. Beck,¹⁸ A. M. Eisner,¹⁸ C. J. Flacco,¹⁸ C. A. Heusch,¹⁸ J. Kroseberg,¹⁸ W. S. Lockman,¹⁸ G. Nesom,¹⁸ T. Schalk,¹⁸ B. A. Schumm,¹⁸ A. Seiden,¹⁸ P. Spradlin,¹⁸ D. C. Williams,¹⁸ M. G. Wilson,¹⁸ J. Albert,¹⁹ E. Chen,¹⁹ A. Dvoretzkii,¹⁹ F. Fang,¹⁹ D. G. Hitlin,¹⁹ I. Narsky,¹⁹ T. Piatenko,¹⁹ F. C. Porter,¹⁹ A. Ryd,¹⁹ A. Samuel,¹⁹ G. Mancinelli,²⁰ B. T. Meadows,²⁰ K. Mishra,²⁰ M. D. Sokoloff,²⁰ F. Blanc,²¹ P. C. Bloom,²¹ S. Chen,²¹ W. T. Ford,²¹ J. F. Hirschauer,²¹ A. Kreisel,²¹ M. Nagel,²¹ U. Nauenberg,²¹ A. Olivas,²¹ W. O. Ruddick,²¹ J. G. Smith,²¹ K. A. Ulmer,²¹ S. R. Wagner,²¹ J. Zhang,²¹ A. Chen,²² E. A. Eckhart,²² A. Soffer,²² W. H. Toki,²² R. J. Wilson,²² F. Winklmeier,²² Q. Zeng,²² D. D. Altenburg,²³ E. Feltresi,²³ A. Hauke,²³ H. Jasper,²³ A. Petzold,²³ B. Spaan,²³ T. Brandt,²⁴ V. Klose,²⁴ H. M. Lacker,²⁴ W. F. Mader,²⁴ R. Nogowski,²⁴ J. Schubert,²⁴ K. R. Schubert,²⁴ R. Schwierz,²⁴ J. E. Sundermann,²⁴ A. Volk,²⁴ D. Bernard,²⁵ G. R. Bonneaud,²⁵ P. Grenier,^{25,*} E. Latour,²⁵ Ch. Thiebaux,²⁵ M. Verderi,²⁵ P. J. Clark,²⁶ W. Gradl,²⁶ F. Muheim,²⁶ S. Playfer,²⁶ A. I. Robertson,²⁶ Y. Xie,²⁶ M. Andreotti,²⁷ D. Bettoni,²⁷ C. Bozzi,²⁷ R. Calabrese,²⁷ G. Cibinetto,²⁷ E. Luppi,²⁷ M. Negrini,²⁷ A. Petrella,²⁷ L. Piemontese,²⁷ E. Prencipe,²⁷ F. Anulli,²⁸ R. Baldini-Ferrolì,²⁸ A. Calcaterra,²⁸ R. de Sangro,²⁸ G. Finocchiaro,²⁸ S. Pacetti,²⁸ P. Patteri,²⁸ I. M. Peruzzi,^{28,†} M. Piccolo,²⁸ M. Rama,²⁸ A. Zallo,²⁸ A. Buzzo,²⁹ R. Capra,²⁹ R. Contri,²⁹ M. Lo Vetere,²⁹ M. M. Macri,²⁹ M. R. Monge,²⁹ S. Passaggio,²⁹ C. Patrignani,²⁹ E. Robutti,²⁹ A. Santroni,²⁹ S. Tosi,²⁹ G. Brandenburg,³⁰ K. S. Chaisanguanthum,³⁰ M. Morii,³⁰ J. Wu,³⁰ R. S. Dubitzky,³¹ J. Marks,³¹ S. Schenk,³¹ U. Uwer,³¹ D. J. Bard,³² W. Bhimji,³² D. A. Bowerman,³² P. D. Dauncey,³² U. Egede,³² R. L. Flack,³² J. A. Nash,³² M. B. Nikolich,³² W. Panduro Vazquez,³² P. K. Behera,³³ X. Chai,³³ M. J. Charles,³³ U. Mallik,³³ N. T. Meyer,³³ V. Ziegler,³³ J. Cochran,³⁴ H. B. Crawley,³⁴ L. Dong,³⁴ V. Eyges,³⁴ W. T. Meyer,³⁴ S. Prell,³⁴ E. I. Rosenberg,³⁴ A. E. Rubin,³⁴ A. V. Gritsan,³⁵ A. G. Denig,³⁶ M. Fritsch,³⁶ G. Schott,³⁶ N. Arnaud,³⁷ M. Davier,³⁷ G. Grosdidier,³⁷ A. Höcker,³⁷ F. Le Diberder,³⁷ V. Lepeltier,³⁷ A. M. Lutz,³⁷ A. Oyanguren,³⁷ S. Pruvot,³⁷ S. Rodier,³⁷ P. Roudeau,³⁷ M. H. Schune,³⁷ A. Stocchi,³⁷ W. F. Wang,³⁷ G. Wormser,³⁷ C. H. Cheng,³⁸ D. J. Lange,³⁸ D. M. Wright,³⁸ C. A. Chavez,³⁹ I. J. Forster,³⁹ J. R. Fry,³⁹ E. Gabathuler,³⁹ R. Gamet,³⁹ K. A. George,³⁹ D. E. Hutchcroft,³⁹ D. J. Payne,³⁹ K. C. Schofield,³⁹ C. Touramanis,³⁹ A. J. Bevan,⁴⁰ F. Di Lodovico,⁴⁰ W. Menges,⁴⁰ R. Sacco,⁴⁰ G. Cowan,⁴¹ H. U. Flaecher,⁴¹ D. A. Hopkins,⁴¹ P. S. Jackson,⁴¹ T. R. McMahon,⁴¹ S. Ricciardi,⁴¹ F. Salvatore,⁴¹ A. C. Wren,⁴¹ D. N. Brown,⁴² C. L. Davis,⁴² J. Allison,⁴³ N. R. Barlow,⁴³ R. J. Barlow,⁴³ Y. M. Chia,⁴³ C. L. Edgar,⁴³ G. D. Lafferty,⁴³ M. T. Naisbit,⁴³ J. C. Williams,⁴³ J. I. Yi,⁴³ C. Chen,⁴⁴ W. D. Hulsbergen,⁴⁴ A. Jawahery,⁴⁴ C. K. Lae,⁴⁴ D. A. Roberts,⁴⁴ G. Simi,⁴⁴ G. Blaylock,⁴⁵ C. Dallapiccola,⁴⁵ S. S. Hertzbach,⁴⁵ X. Li,⁴⁵ T. B. Moore,⁴⁵ S. Saremi,⁴⁵ H. Staengle,⁴⁵ R. Cowan,⁴⁶ G. Sciolla,⁴⁶ S. J. Sekula,⁴⁶ M. Spitznagel,⁴⁶ F. Taylor,⁴⁶ R. K. Yamamoto,⁴⁶ H. Kim,⁴⁷

S. E. Mclachlin,⁴⁷ P. M. Patel,⁴⁷ S. H. Robertson,⁴⁷ A. Lazzaro,⁴⁸ V. Lombardo,⁴⁸ F. Palombo,⁴⁸ J. M. Bauer,⁴⁹ L. Cremaldi,⁴⁹ V. Eschenburg,⁴⁹ R. Godang,⁴⁹ R. Kroeger,⁴⁹ D. A. Sanders,⁴⁹ D. J. Summers,⁴⁹ H. W. Zhao,⁴⁹ S. Brunet,⁵⁰ D. Côté,⁵⁰ M. Simard,⁵⁰ P. Taras,⁵⁰ F. B. Viaud,⁵⁰ H. Nicholson,⁵¹ N. Cavallo,^{52, †} G. De Nardo,⁵² F. Fabozzi,^{52, †} C. Gatto,⁵² L. Lista,⁵² D. Monorchio,⁵² P. Paolucci,⁵² D. Piccolo,⁵² C. Sciacca,⁵² M. Baak,⁵³ G. Raven,⁵³ H. L. Snoek,⁵³ C. P. Jessop,⁵⁴ J. M. LoSecco,⁵⁴ T. Allmendinger,⁵⁵ G. Benelli,⁵⁵ K. K. Gan,⁵⁵ K. Honscheid,⁵⁵ D. Hufnagel,⁵⁵ P. D. Jackson,⁵⁵ H. Kagan,⁵⁵ R. Kass,⁵⁵ A. M. Rahimi,⁵⁵ R. Ter-Antonyan,⁵⁵ Q. K. Wong,⁵⁵ N. L. Blount,⁵⁶ J. Brau,⁵⁶ R. Frey,⁵⁶ O. Igonkina,⁵⁶ M. Lu,⁵⁶ R. Rahmat,⁵⁶ N. B. Sinev,⁵⁶ D. Strom,⁵⁶ J. Strube,⁵⁶ E. Torrence,⁵⁶ A. Gaz,⁵⁷ M. Margoni,⁵⁷ M. Morandin,⁵⁷ A. Pompili,⁵⁷ M. Posocco,⁵⁷ M. Rotondo,⁵⁷ F. Simonetto,⁵⁷ R. Stroili,⁵⁷ C. Voci,⁵⁷ M. Benayoun,⁵⁸ J. Chauveau,⁵⁸ H. Briand,⁵⁸ P. David,⁵⁸ L. Del Buono,⁵⁸ Ch. de la Vaissière,⁵⁸ O. Hamon,⁵⁸ B. L. Hartfiel,⁵⁸ M. J. J. John,⁵⁸ Ph. Leruste,⁵⁸ J. Malclès,⁵⁸ J. Ocariz,⁵⁸ L. Roos,⁵⁸ G. Therin,⁵⁸ L. Gladney,⁵⁹ J. Panetta,⁵⁹ M. Biasini,⁶⁰ R. Covarelli,⁶⁰ C. Angelini,⁶¹ G. Batignani,⁶¹ S. Bettarini,⁶¹ F. Bucci,⁶¹ G. Calderini,⁶¹ M. Carpinelli,⁶¹ R. Cenci,⁶¹ F. Forti,⁶¹ M. A. Giorgi,⁶¹ A. Lusiani,⁶¹ G. Marchiori,⁶¹ M. A. Mazur,⁶¹ M. Morganti,⁶¹ N. Neri,⁶¹ E. Paoloni,⁶¹ G. Rizzo,⁶¹ J. J. Walsh,⁶¹ M. Haire,⁶² D. Judd,⁶² D. E. Wagoner,⁶² J. Biesiada,⁶³ N. Danielson,⁶³ P. Elmer,⁶³ Y. P. Lau,⁶³ C. Lu,⁶³ J. Olsen,⁶³ A. J. S. Smith,⁶³ A. V. Telnov,⁶³ F. Bellini,⁶⁴ G. Cavoto,⁶⁴ A. D’Orazio,⁶⁴ D. del Re,⁶⁴ E. Di Marco,⁶⁴ R. Faccini,⁶⁴ F. Ferrarotto,⁶⁴ F. Ferroni,⁶⁴ M. Gaspero,⁶⁴ L. Li Gioi,⁶⁴ M. A. Mazzoni,⁶⁴ S. Morganti,⁶⁴ G. Piredda,⁶⁴ F. Polci,⁶⁴ F. Safai Tehrani,⁶⁴ C. Voena,⁶⁴ M. Ebert,⁶⁵ H. Schröder,⁶⁵ R. Waldi,⁶⁵ T. Adye,⁶⁶ N. De Groot,⁶⁶ B. Franek,⁶⁶ E. O. Olaiya,⁶⁶ F. F. Wilson,⁶⁶ R. Aleksan,⁶⁷ S. Emery,⁶⁷ A. Gaidot,⁶⁷ S. F. Ganzhur,⁶⁷ G. Hamel de Monchenault,⁶⁷ W. Kozanecki,⁶⁷ M. Legendre,⁶⁷ G. Vasseur,⁶⁷ Ch. Yèche,⁶⁷ M. Zito,⁶⁷ X. R. Chen,⁶⁸ H. Liu,⁶⁸ W. Park,⁶⁸ M. V. Purohit,⁶⁸ J. R. Wilson,⁶⁸ M. T. Allen,⁶⁹ D. Aston,⁶⁹ R. Bartoldus,⁶⁹ P. Bechtle,⁶⁹ N. Berger,⁶⁹ R. Claus,⁶⁹ J. P. Coleman,⁶⁹ M. R. Convery,⁶⁹ M. Cristinziani,⁶⁹ J. C. Dingfelder,⁶⁹ J. Dorfan,⁶⁹ G. P. Dubois-Felsmann,⁶⁹ D. Dujmic,⁶⁹ W. Dunwoodie,⁶⁹ R. C. Field,⁶⁹ T. Glanzman,⁶⁹ S. J. Gowdy,⁶⁹ M. T. Graham,⁶⁹ V. Halyo,⁶⁹ C. Hast,⁶⁹ T. Hryn’ova,⁶⁹ W. R. Innes,⁶⁹ M. H. Kelsey,⁶⁹ P. Kim,⁶⁹ D. W. G. S. Leith,⁶⁹ S. Li,⁶⁹ S. Luitz,⁶⁹ V. Luth,⁶⁹ H. L. Lynch,⁶⁹ D. B. MacFarlane,⁶⁹ H. Marsiske,⁶⁹ R. Messner,⁶⁹ D. R. Muller,⁶⁹ C. P. O’Grady,⁶⁹ V. E. Ozcan,⁶⁹ A. Perazzo,⁶⁹ M. Perl,⁶⁹ T. Pulliam,⁶⁹ B. N. Ratcliff,⁶⁹ A. Roodman,⁶⁹ A. A. Salnikov,⁶⁹ R. H. Schindler,⁶⁹ J. Schwiening,⁶⁹ A. Snyder,⁶⁹ J. Stelzer,⁶⁹ D. Su,⁶⁹ M. K. Sullivan,⁶⁹ K. Suzuki,⁶⁹ S. K. Swain,⁶⁹ J. M. Thompson,⁶⁹ J. Va’vra,⁶⁹ N. van Bakel,⁶⁹ M. Weaver,⁶⁹ A. J. R. Weinstein,⁶⁹ W. J. Wisniewski,⁶⁹ M. Wittgen,⁶⁹ D. H. Wright,⁶⁹ A. K. Yarritu,⁶⁹ K. Yi,⁶⁹ C. C. Young,⁶⁹ P. R. Burchat,⁷⁰ A. J. Edwards,⁷⁰ S. A. Majewski,⁷⁰ B. A. Petersen,⁷⁰ C. Roat,⁷⁰ L. Wilden,⁷⁰ S. Ahmed,⁷¹ M. S. Alam,⁷¹ R. Bula,⁷¹ J. A. Ernst,⁷¹ V. Jain,⁷¹ B. Pan,⁷¹ M. A. Saeed,⁷¹ F. R. Wappler,⁷¹ S. B. Zain,⁷¹ W. Bugg,⁷² M. Krishnamurthy,⁷² S. M. Spanier,⁷² R. Eckmann,⁷³ J. L. Ritchie,⁷³ A. Satpathy,⁷³ C. J. Schilling,⁷³ R. F. Schwitters,⁷³ J. M. Izen,⁷⁴ X. C. Lou,⁷⁴ S. Ye,⁷⁴ F. Bianchi,⁷⁵ F. Gallo,⁷⁵ D. Gamba,⁷⁵ M. Bomben,⁷⁶ L. Bosisio,⁷⁶ C. Cartaro,⁷⁶ F. Cossutti,⁷⁶ G. Della Ricca,⁷⁶ S. Dittongo,⁷⁶ L. Lanceri,⁷⁶ L. Vitale,⁷⁶ V. Azzolini,⁷⁷ F. Martinez-Vidal,⁷⁷ Sw. Banerjee,⁷⁸ B. Bhuyan,⁷⁸ C. M. Brown,⁷⁸ D. Fortin,⁷⁸ K. Hamano,⁷⁸ R. Kowalewski,⁷⁸ I. M. Nugent,⁷⁸ J. M. Roney,⁷⁸ R. J. Sobie,⁷⁸ J. J. Back,⁷⁹ P. F. Harrison,⁷⁹ T. E. Latham,⁷⁹ G. B. Mohanty,⁷⁹ M. Pappagallo,⁷⁹ H. R. Band,⁸⁰ X. Chen,⁸⁰ B. Cheng,⁸⁰ S. Dasu,⁸⁰ M. Datta,⁸⁰ K. T. Flood,⁸⁰ J. J. Hollar,⁸⁰ P. E. Kutter,⁸⁰ B. Mellado,⁸⁰ A. Mihalyi,⁸⁰ Y. Pan,⁸⁰ M. Pierini,⁸⁰ R. Prepost,⁸⁰ S. L. Wu,⁸⁰ Z. Yu,⁸⁰ and H. Neal⁸¹

(The BABAR Collaboration)

¹Laboratoire de Physique des Particules, F-74941 Annecy-le-Vieux, France

²Universitat de Barcelona, Facultat de Fisica Dept. ECM, E-08028 Barcelona, Spain

³Università di Bari, Dipartimento di Fisica and INFN, I-70126 Bari, Italy

⁴Institute of High Energy Physics, Beijing 100039, China

⁵University of Bergen, Institute of Physics, N-5007 Bergen, Norway

⁶Lawrence Berkeley National Laboratory and University of California, Berkeley, California 94720, USA

⁷University of Birmingham, Birmingham, B15 2TT, United Kingdom

⁸Ruhr Universität Bochum, Institut für Experimentalphysik 1, D-44780 Bochum, Germany

⁹University of Bristol, Bristol BS8 1TL, United Kingdom

¹⁰University of British Columbia, Vancouver, British Columbia, Canada V6T 1Z1

¹¹Brunel University, Uxbridge, Middlesex UB8 3PH, United Kingdom

¹²Budker Institute of Nuclear Physics, Novosibirsk 630090, Russia

¹³University of California at Irvine, Irvine, California 92697, USA

¹⁴University of California at Los Angeles, Los Angeles, California 90024, USA

¹⁵University of California at Riverside, Riverside, California 92521, USA

¹⁶University of California at San Diego, La Jolla, California 92093, USA

- ¹⁷University of California at Santa Barbara, Santa Barbara, California 93106, USA
- ¹⁸University of California at Santa Cruz, Institute for Particle Physics, Santa Cruz, California 95064, USA
- ¹⁹California Institute of Technology, Pasadena, California 91125, USA
- ²⁰University of Cincinnati, Cincinnati, Ohio 45221, USA
- ²¹University of Colorado, Boulder, Colorado 80309, USA
- ²²Colorado State University, Fort Collins, Colorado 80523, USA
- ²³Universität Dortmund, Institut für Physik, D-44221 Dortmund, Germany
- ²⁴Technische Universität Dresden, Institut für Kern- und Teilchenphysik, D-01062 Dresden, Germany
- ²⁵Ecole Polytechnique, Laboratoire Leprince-Ringuet, F-91128 Palaiseau, France
- ²⁶University of Edinburgh, Edinburgh EH9 3JZ, United Kingdom
- ²⁷Università di Ferrara, Dipartimento di Fisica and INFN, I-44100 Ferrara, Italy
- ²⁸Laboratori Nazionali di Frascati dell'INFN, I-00044 Frascati, Italy
- ²⁹Università di Genova, Dipartimento di Fisica and INFN, I-16146 Genova, Italy
- ³⁰Harvard University, Cambridge, Massachusetts 02138, USA
- ³¹Universität Heidelberg, Physikalisches Institut, Philosophenweg 12, D-69120 Heidelberg, Germany
- ³²Imperial College London, London, SW7 2AZ, United Kingdom
- ³³University of Iowa, Iowa City, Iowa 52242, USA
- ³⁴Iowa State University, Ames, Iowa 50011-3160, USA
- ³⁵Johns Hopkins University, Baltimore, Maryland 21218, USA
- ³⁶Universität Karlsruhe, Institut für Experimentelle Kernphysik, D-76021 Karlsruhe, Germany
- ³⁷Laboratoire de l'Accélérateur Linéaire, IN2P3-CNRS et Université Paris-Sud 11, Centre Scientifique d'Orsay, B.P. 34, F-91898 ORSAY Cedex, France
- ³⁸Lawrence Livermore National Laboratory, Livermore, California 94550, USA
- ³⁹University of Liverpool, Liverpool L69 7ZE, United Kingdom
- ⁴⁰Queen Mary, University of London, E1 4NS, United Kingdom
- ⁴¹University of London, Royal Holloway and Bedford New College, Egham, Surrey TW20 0EX, United Kingdom
- ⁴²University of Louisville, Louisville, Kentucky 40292, USA
- ⁴³University of Manchester, Manchester M13 9PL, United Kingdom
- ⁴⁴University of Maryland, College Park, Maryland 20742, USA
- ⁴⁵University of Massachusetts, Amherst, Massachusetts 01003, USA
- ⁴⁶Massachusetts Institute of Technology, Laboratory for Nuclear Science, Cambridge, Massachusetts 02139, USA
- ⁴⁷McGill University, Montréal, Québec, Canada H3A 2T8
- ⁴⁸Università di Milano, Dipartimento di Fisica and INFN, I-20133 Milano, Italy
- ⁴⁹University of Mississippi, University, Mississippi 38677, USA
- ⁵⁰Université de Montréal, Physique des Particules, Montréal, Québec, Canada H3C 3J7
- ⁵¹Mount Holyoke College, South Hadley, Massachusetts 01075, USA
- ⁵²Università di Napoli Federico II, Dipartimento di Scienze Fisiche and INFN, I-80126, Napoli, Italy
- ⁵³NIKHEF, National Institute for Nuclear Physics and High Energy Physics, NL-1009 DB Amsterdam, The Netherlands
- ⁵⁴University of Notre Dame, Notre Dame, Indiana 46556, USA
- ⁵⁵Ohio State University, Columbus, Ohio 43210, USA
- ⁵⁶University of Oregon, Eugene, Oregon 97403, USA
- ⁵⁷Università di Padova, Dipartimento di Fisica and INFN, I-35131 Padova, Italy
- ⁵⁸Universités Paris VI et VII, Laboratoire de Physique Nucléaire et de Hautes Energies, F-75252 Paris, France
- ⁵⁹University of Pennsylvania, Philadelphia, Pennsylvania 19104, USA
- ⁶⁰Università di Perugia, Dipartimento di Fisica and INFN, I-06100 Perugia, Italy
- ⁶¹Università di Pisa, Dipartimento di Fisica, Scuola Normale Superiore and INFN, I-56127 Pisa, Italy
- ⁶²Prairie View A&M University, Prairie View, Texas 77446, USA
- ⁶³Princeton University, Princeton, New Jersey 08544, USA
- ⁶⁴Università di Roma La Sapienza, Dipartimento di Fisica and INFN, I-00185 Roma, Italy
- ⁶⁵Universität Rostock, D-18051 Rostock, Germany
- ⁶⁶Rutherford Appleton Laboratory, Chilton, Didcot, Oxon, OX11 0QX, United Kingdom
- ⁶⁷DSM/Dapnia, CEA/Saclay, F-91191 Gif-sur-Yvette, France
- ⁶⁸University of South Carolina, Columbia, South Carolina 29208, USA
- ⁶⁹Stanford Linear Accelerator Center, Stanford, California 94309, USA
- ⁷⁰Stanford University, Stanford, California 94305-4060, USA
- ⁷¹State University of New York, Albany, New York 12222, USA
- ⁷²University of Tennessee, Knoxville, Tennessee 37996, USA
- ⁷³University of Texas at Austin, Austin, Texas 78712, USA
- ⁷⁴University of Texas at Dallas, Richardson, Texas 75083, USA
- ⁷⁵Università di Torino, Dipartimento di Fisica Sperimentale and INFN, I-10125 Torino, Italy
- ⁷⁶Università di Trieste, Dipartimento di Fisica and INFN, I-34127 Trieste, Italy
- ⁷⁷IFIC, Universitat de Valencia-CSIC, E-46071 Valencia, Spain
- ⁷⁸University of Victoria, Victoria, British Columbia, Canada V8W 3P6
- ⁷⁹Department of Physics, University of Warwick, Coventry CV4 7AL, United Kingdom

⁸⁰University of Wisconsin, Madison, Wisconsin 53706, USA

⁸¹Yale University, New Haven, Connecticut 06511, USA

(Dated: October 25, 2018)

We report a measurement of the $B \rightarrow \pi \ell \nu$ branching fraction based on 211 fb^{-1} of data collected with the *BABAR* detector. We use samples of B^0 and B^+ mesons tagged by a second B meson reconstructed in a semileptonic or hadronic decay, and combine the results assuming isospin symmetry to obtain $\mathcal{B}(B^0 \rightarrow \pi^- \ell^+ \nu) = (1.33 \pm 0.17_{\text{stat}} \pm 0.11_{\text{syst}}) \times 10^{-4}$. We determine the magnitude of the Cabibbo-Kobayashi-Maskawa matrix element $|V_{ub}|$ by combining the partial branching fractions measured in ranges of the momentum transfer squared and theoretical calculations of the form factor. Using a recent lattice QCD calculation, we find $|V_{ub}| = (4.5 \pm 0.5_{\text{stat}} \pm 0.3_{\text{syst}}^{+0.7}_{-0.5 \text{ FF}}) \times 10^{-3}$, where the last error is due to the normalization of the form factor.

PACS numbers: 13.20.He, 12.15.Hh, 12.38.Qk, 14.40.Nd

The magnitude of the Cabibbo-Kobayashi-Maskawa matrix [1] element V_{ub} is a critical constraint on the Unitarity Triangle. Our knowledge of $|V_{ub}|$ comes from measurements of the $b \rightarrow u \ell \nu$ decay rate, where the hadronic system in the final state can be reconstructed either inclusively or exclusively. The precisions are limited by the uncertainties in the non-perturbative QCD calculations that are used to extract $|V_{ub}|$ from the measured decay rates. It is therefore crucial to pursue both the inclusive and exclusive approaches, which rely on different theoretical methods, and to test their consistency.

The rate of the exclusive decay $B \rightarrow \pi \ell \nu$ ($\ell = e$ or μ) is related to $|V_{ub}|$ through the form factor $f_+(q^2)$, where q^2 is the momentum transfer squared. Measurements of the $B \rightarrow \pi \ell \nu$ branching fraction have been reported by CLEO [2], *BABAR* [3], and Belle [4]. In this Letter, we report a measurement in which $B \rightarrow \pi \ell \nu$ decays are searched for in $\Upsilon(4S) \rightarrow B\bar{B}$ events that are identified by reconstruction of the second B meson (B_{tag}). The technique, which was also used in [4], allows us to constrain the kinematics, reduce the combinatorics, and determine the charge of the signal B . The result is an improved signal purity at the expense of the efficiency compared with the traditional measurements in which only the signal B meson is reconstructed. We perform two analyses in which B_{tag} is reconstructed in semileptonic and hadronic decays, respectively, and combine the measured partial branching fractions $\Delta\mathcal{B}$ in ranges of q^2 with the recent form-factor calculations [5, 6, 7, 8] to determine $|V_{ub}|$.

The measurement uses a sample of approximately 232 million $B\bar{B}$ pairs, corresponding to an integrated luminosity of 211 fb^{-1} , recorded near the $\Upsilon(4S)$ resonance with the *BABAR* detector [9] at the PEP-II asymmetric-energy e^+e^- storage rings. We use a detailed Monte Carlo (MC) simulation to estimate the signal efficiency and the signal and background distributions.

In the first analysis, we reconstruct B_{tag} in the semileptonic decay $B \rightarrow D^{(*)} \ell \nu$. We reconstruct D^0 mesons in $K^-\pi^+$, $K^-\pi^+\pi^+\pi^-$, $K^-\pi^+\pi^0$, and $K_S^0\pi^+\pi^-$ decays, and D^+ mesons in $K^-\pi^+\pi^+$ decays [10]. The D mass resolution (σ) is between 4.6 and 12.9 MeV depending on the decay channel. The mass of the D candidate

is required to be within 2.6σ and 3.0σ of the expected value for the B^0 and B^+ channels, respectively. We also use a sideband sample, in which the D candidate mass is more than 3σ away from the nominal value, for subtracting the combinatoric background. We reconstruct D^{*+} mesons in $D^0\pi^+$ and $D^+\pi^0$ decays. The mass difference between the D^* and D is required to be within 3 MeV of the expected value [11]. The reconstructed D and D^* candidates are paired with a charged lepton with a center-of-mass (c.m.) momentum $|\mathbf{p}_\ell| > 0.8 \text{ GeV}$ to form a $Y = D^{(*)}\ell$ system. If the D decay contains a charged kaon, the lepton must have the same charge as the kaon. The lepton and the D meson are required to originate from a common vertex. Assuming that only a massless neutrino escaped detection, we calculate the cosine of the angle between the B and Y momenta as $\cos\theta_{BY} = (2E_B E_Y - m_B^2 - m_Y^2)/(2|\mathbf{p}_B||\mathbf{p}_Y|)$, where m_B , m_Y , E_B , E_Y , \mathbf{p}_B , \mathbf{p}_Y refer to the masses, c.m. energies, and momenta of the B and Y , respectively. For background events, $\cos\theta_{BY}$ does not correspond to the cosine of a physical angle and can extend outside ± 1 . We apply a loose selection of $|\cos\theta_{BY}| < 5$ at this stage.

After identifying the B_{tag} meson, we require the remaining particles in the event to be consistent with a $B \rightarrow \pi \ell \nu$ decay. Charged tracks that are not identified as a lepton or a kaon are considered charged pion candidates. Neutral pion candidates are formed from pairs of photon candidates with invariant mass between 115 and 150 MeV. For the B^0 channel, the lepton must have $|\mathbf{p}_\ell| > 0.8 \text{ GeV}$, and its charge must be opposite to that of the charged pion. The lepton charge must be opposite to that of the B_{tag} for the B^+ channel. We reject the lepton candidate if, when combined with an oppositely-charged track, it is consistent with a $J/\psi \rightarrow \ell^+\ell^-$ decay or a photon conversion. Once the signal B candidate is identified, we require that the event contain no other charged particles and small total c.m. energy E_{res} of the residual neutral particles. In measuring E_{res} , we remove the neutral candidates that are consistent with coming from a $D^* \rightarrow D\pi^0$ or $D\gamma$ decay, bremsstrahlung from an electron, or beam-related background. We require $E_{\text{res}} < 70 \text{ MeV}$ for the B^0 chan-

nel and $E_{\text{res}} < 250$ MeV for the B^+ channel, the latter being relaxed to allow for additional photons from decays of D^{*0} and higher resonances. We calculate the cosine of the angle between the B and $\pi\ell$ momenta as $\cos\theta_{B\pi\ell} = (2E_B E_{\pi\ell} - m_B^2 - m_{\pi\ell}^2)/(2|\mathbf{p}_B||\mathbf{p}_{\pi\ell}|)$, where $m_{\pi\ell}$, $E_{\pi\ell}$, $\mathbf{p}_{\pi\ell}$ are the mass, c.m. energy, and momentum of the $\pi\ell$ system, respectively. We require $|\cos\theta_{B\pi\ell}| < 5$.

Ignoring the small c.m. momentum of the B meson, the invariant mass squared of the lepton-neutrino system in a $B \rightarrow \pi\ell\nu$ decay can be inferred as $q^2 = (m_B - E_\pi)^2 - |\mathbf{p}_\pi|^2$, where E_π and \mathbf{p}_π are the c.m. energy and momentum of the pion. We divide the data into three bins: $q^2 < 8$ GeV², $8 < q^2 < 16$ GeV², and $q^2 > 16$ GeV². We use simulated $B \rightarrow \pi\ell\nu$ events to estimate and to correct for the small ($< 8\%$) migration between the q^2 bins due to resolution, which is approximately 0.8 GeV² at $q^2 = 8$ GeV² and improves with increasing q^2 .

Having identified the two B mesons that decayed semileptonically, conservation of the total momentum determines the angle ϕ_B between the direction of the B momenta and the plane defined by the Y and $\pi\ell$ momenta:

$$\cos^2\phi_B = \frac{\cos^2\theta_{BY} + \cos^2\theta_{B\pi\ell} + 2\cos\theta_{BY}\cos\theta_{B\pi\ell}\cos\gamma}{\sin^2\gamma}, \quad (1)$$

where γ is the angle between the Y and $\pi\ell$ momenta. The variable $\cos^2\phi_B$ satisfies $\cos^2\phi_B \leq 1$ for correctly reconstructed signal events, and is broadly distributed for the background (see Fig. 1). We use the $\cos^2\phi_B$ distributions to extract the signal yield in the data in each q^2 bin. We did not require stringent cuts on $\cos\theta_{BY}$ and $\cos\theta_{B\pi\ell}$ because they are incorporated in $\cos^2\phi_B$.

We express the data distribution as a sum of three contributions: $dN/d\cos^2\phi_B = N_{\text{sig}}\mathcal{P}_{\text{sig}} + N_{\text{bkg}}\mathcal{P}_{\text{bkg}} + N_{\text{cmb}}\mathcal{P}_{\text{cmb}}$, where N_c and \mathcal{P}_c are the number of events and the probability density function (PDF) for each category c , defined as the signal (sig), background with correctly-reconstructed D mesons (bkg), and other backgrounds (cmb). The events in the D mass sideband are also used in the fit to constrain the $N_{\text{cmb}}\mathcal{P}_{\text{cmb}}$ term. The PDF shapes are determined from the MC simulation. The signal PDF is a combination of a smeared step function and an exponential tail. The background PDFs are either an exponential plus constant or a second order polynomial. The two data samples (D mass peak and sideband) and the MC samples are used in an unbinned maximum likelihood fit that determines N_{sig} , N_{bkg} , N_{cmb} , and the PDF parameters simultaneously. Figure 1 shows the fit results summed over the q^2 bins. We find the signal yields and their statistical errors to be 57_{-12}^{+13} events and 92_{-24}^{+26} events for the B^0 and B^+ channels, respectively.

We use simulated $B \rightarrow \pi\ell\nu$ events to estimate the signal efficiencies. Control samples are used to derive corrections for the data-MC differences in the B_{tag} reconstruction, charged and neutral particle reconstruc-

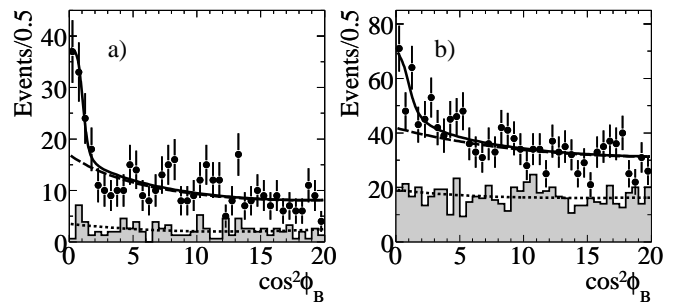


FIG. 1: Distributions of $\cos^2\phi_B$ of the a) $B^0 \rightarrow \pi^-\ell^+\nu$ and b) $B^+ \rightarrow \pi^0\ell^+\nu$ candidates. The points with error bars and the shaded histograms are the data in the D mass peak and sideband, respectively. The curves are the fit results representing the total (solid), background (dashed), and ‘cmb’ (dotted) components defined in the text. The fits were performed in bins of q^2 , but the results shown are for the complete q^2 range.

tion, and lepton identification. The largest uncertainty comes from the B_{tag} reconstruction efficiency, which is determined from a sample of events in which two non-overlapping B_{tag} candidates are reconstructed. The efficiency correction factors for the B_{tag} reconstruction are found to be 1.00 ± 0.07 and 0.99 ± 0.02 for the B^0 and B^+ channels, respectively. The average signal efficiencies after the correction are 1.1×10^{-3} for the B^0 channel and 3.0×10^{-3} for the B^+ channel. The latter is larger mainly because of the higher efficiency of reconstructing a D^0 meson compared with a D^+ or D^{*+} meson.

The measured branching fractions are summarized in Table I. The largest sources of systematic error [12] are: the B_{tag} reconstruction efficiency (discussed above), the shape of the background $\cos^2\phi_B$ distribution (studied with control samples that fail the signal selection criteria), and the branching fractions of the B semileptonic decays other than $B \rightarrow \pi\ell\nu$ (varied within the current knowledge [11]).

In the second analysis, we reconstruct the B_{tag} meson in a set of purely hadronic final states $B \rightarrow D^{(*)}X$. We reconstruct D^0 mesons in $K^-\pi^+$, $K^-\pi^+\pi^0$, $K^-\pi^+\pi^+\pi^-$, and $K_s^0\pi^+\pi^-$ decays, and D^+ mesons in $K^-\pi^+\pi^+$, $K^-\pi^+\pi^+\pi^0$, $K_s^0\pi^+$, $K_s^0\pi^+\pi^0$, and $K_s^0\pi^+\pi^+\pi^-$ decays. The D^* mesons are reconstructed in $D^0\pi^+$, $D^0\pi^0$, and $D^0\gamma$ decays. The hadronic system X has a total charge ± 1 and is composed of $n_1\pi^\pm + n_2K^\pm + n_3\pi^0 + n_4K_s^0$ where $n_1 + n_2 < 6$, $n_3 < 3$ and $n_4 < 3$. The total reconstruction efficiency for a B^0 (B^+) meson is 0.3% (0.5%).

We separate correctly-reconstructed B_{tag} mesons from the background using two kinematic variables: the beam-energy substituted mass $m_{\text{ES}} = \sqrt{s/4 - |\mathbf{p}_B|^2}$ and the energy difference $\Delta E = E_B - \sqrt{s}/2$, where \sqrt{s} is the c.m. energy of the e^+e^- system. We select signal candidates in mode-dependent ΔE windows around zero. We apply a loose selection $5.2 < m_{\text{ES}} < 5.3$ GeV and fit the m_{ES} distribution at a later stage to extract the signal yield.

TABLE I: Partial and total branching fractions, in units of 10^{-4} , measured with the semileptonic and hadronic tag analyses. The q^2 ranges are in GeV^2 . The errors are statistical and systematic. The combined results are expressed as $B^0 \rightarrow \pi^- \ell^+ \nu$ branching fractions.

		$q^2 < 8$	$8 < q^2 < 16$	$q^2 > 16$	$q^2 < 16$	Total
B^0	Semileptonic	$0.50 \pm 0.16 \pm 0.05$	$0.33 \pm 0.14 \pm 0.04$	$0.29 \pm 0.15 \pm 0.04$	$0.83 \pm 0.22 \pm 0.08$	$1.12 \pm 0.25 \pm 0.10$
	Hadronic	$0.09 \pm 0.10 \pm 0.02$	$0.33 \pm 0.15 \pm 0.05$	$0.65 \pm 0.20 \pm 0.13$	$0.42 \pm 0.18 \pm 0.05$	$1.07 \pm 0.27 \pm 0.15$
	Average	$0.38 \pm 0.12 \pm 0.04$	$0.33 \pm 0.10 \pm 0.03$	$0.47 \pm 0.13 \pm 0.06$	$0.72 \pm 0.16 \pm 0.06$	$1.19 \pm 0.20 \pm 0.10$
B^+	Semileptonic	$0.18 \pm 0.08 \pm 0.02$	$0.45 \pm 0.13 \pm 0.05$	$0.10 \pm 0.12 \pm 0.04$	$0.63 \pm 0.16 \pm 0.06$	$0.73 \pm 0.18 \pm 0.08$
	Hadronic	$0.16 \pm 0.11 \pm 0.03$	$0.39 \pm 0.16 \pm 0.06$	$0.26 \pm 0.12 \pm 0.06$	$0.56 \pm 0.19 \pm 0.08$	$0.82 \pm 0.22 \pm 0.11$
	Average	$0.18 \pm 0.07 \pm 0.02$	$0.43 \pm 0.10 \pm 0.04$	$0.22 \pm 0.09 \pm 0.05$	$0.61 \pm 0.12 \pm 0.05$	$0.82 \pm 0.15 \pm 0.09$
Combined	$0.36 \pm 0.09 \pm 0.03$	$0.52 \pm 0.10 \pm 0.04$	$0.46 \pm 0.10 \pm 0.06$	$0.87 \pm 0.13 \pm 0.06$	$1.33 \pm 0.17 \pm 0.11$	

After reconstructing the B_{tag} , we look for the signature of a $B \rightarrow \pi \ell \nu$ decay in the recoiling system. The selection criteria for the pion and lepton candidates are similar to the first analysis, except a) the minimum $|\mathbf{p}_\ell|$ for electrons is 0.5 GeV , and b) the π^0 mass window is $110\text{--}160 \text{ MeV}$. We require $E_{\text{res}} < 450 \text{ MeV}$ for the B^0 channel to reduce the $B^0 \rightarrow \rho^- \ell^+ \nu$ background, and no requirement is made for the B^+ channel.

The full reconstruction of B_{tag} allows us to determine the neutrino four-momentum precisely from the missing four-momentum $p_{\text{miss}} = p_{\mathcal{R}(4S)} - p_{B_{\text{tag}}} - p_\pi - p_\ell$. The missing mass squared m_{miss}^2 peaks near zero for the signal and extends above zero for the background (see Fig. 2). We require $|m_{\text{miss}}^2| < 0.3 \text{ GeV}^2$ for the B^0 channel and $-0.5 < m_{\text{miss}}^2 < 0.7 \text{ GeV}^2$ for the B^+ channel, with the latter being broader and asymmetric due to the resolution of the π^0 energy measurement.

Precise knowledge of p_{miss} allows us to calculate q^2 with small uncertainties. We divide the signal candidates into the same three q^2 bins as before, and subtract the small bin-to-bin migration as background. In each q^2 bin, we obtain the number of correctly-tagged events by an unbinned maximum likelihood fit to the m_{ES} distribution. The PDF for the signal is determined from MC simulation as a Gaussian function joined to an exponential tail. For the background, we use a threshold function of the form $x\sqrt{1-x^2}\exp(-\xi(1-x^2))$, where $x = 2m_{\text{ES}}/\sqrt{s}$ and the parameter ξ is allowed to float in the fit. Fig. 2 shows the m_{miss}^2 distribution obtained by splitting the data samples in bins of m_{miss}^2 and repeating the m_{ES} fit.

The signal side of the correctly-tagged events may not be a $B \rightarrow \pi \ell \nu$ decay. Contributions from this type of background are estimated with the MC simulation, as indicated by shaded histograms in Fig. 2, which are scaled to match the data in the sideband region $1 < m_{\text{miss}}^2 < 4 \text{ GeV}^2$. After background subtraction, we find signal yields of 31 ± 7 events and 26 ± 7 events for the B^0 and B^+ channels, respectively, where the errors are statistical.

Instead of estimating the absolute signal efficiency, we

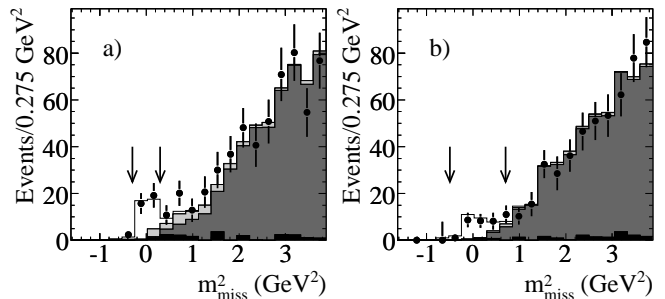


FIG. 2: Distributions of m_{miss}^2 of the a) $B^0 \rightarrow \pi^- \ell^+ \nu$ and b) $B^+ \rightarrow \pi^0 \ell^+ \nu$ candidates. The points with error bars are the data. The histograms represent, from the lightest to the darkest, the MC simulation of the $B \rightarrow \pi \ell \nu$ signal, $b \rightarrow u \ell \nu$, $b \rightarrow c \ell \nu$, and other backgrounds. The arrows indicate the regions in which the signals are extracted.

normalize the signal yield to the number of inclusive B semileptonic decays, $B \rightarrow X \ell \nu$, in the recoil of B_{tag} . The reconstruction efficiencies of the B_{tag} and of the lepton cancel to first order in the ratio between the yields of the signal and normalization samples. The inclusive branching fraction $\mathcal{B}(B \rightarrow X \ell \nu)$ is taken as $10.73 \pm 0.28\%$ [11]. The yield of the normalization sample is extracted by a fit to the m_{ES} distribution. The component of the background that peaks in the m_{ES} distribution is estimated from the MC simulation and subtracted. Efficiency differences between the signal and normalization samples are estimated with the MC simulation, and the corresponding corrections are applied to the result.

The measured branching fractions are summarized in Table I. The largest source of systematic error is the limited statistics of the signal MC sample. Other significant sources include the modeling of the signal PDF (studied with alternative fitting methods), photon-energy measurement, π^0 reconstruction, muon identification, and the branching fractions of non-signal $B \rightarrow X_u \ell \nu$ decays.

We take weighted averages of the measured partial branching fractions in each q^2 bin. The results for the B^0 and B^+ channels are consistent with the isospin relation $\Gamma(B^0 \rightarrow \pi^- \ell^+ \nu) = 2\Gamma(B^+ \rightarrow \pi^0 \ell^+ \nu)$ and the lifetime

TABLE II: Values of $|V_{ub}|$ derived using the form factor calculations. The first two errors on $|V_{ub}|$ come from the statistical and systematic uncertainties of the partial branching fractions. The third errors correspond to the uncertainties on $\Delta\zeta$ due to the form-factor calculations, and are taken from Refs. 5, 6, 7, 8.

	q^2 (GeV ²)	$\Delta\zeta$ (ps ⁻¹)	$ V_{ub} $ (10 ⁻³)
Ball-Zwicky [5]	< 16	5.44 ± 1.43	$3.2 \pm 0.2 \pm 0.1^{+0.5}_{-0.4}$
Gulez <i>et al.</i> [6]	> 16	1.46 ± 0.35	$4.5 \pm 0.5 \pm 0.3^{+0.7}_{-0.5}$
Okamoto <i>et al.</i> [7]	> 16	1.83 ± 0.50	$4.0 \pm 0.5 \pm 0.3^{+0.7}_{-0.5}$
Abada <i>et al.</i> [8]	> 16	1.80 ± 0.86	$4.1 \pm 0.5 \pm 0.3^{+1.6}_{-0.7}$

ratio $\tau_{B^+}/\tau_{B^0} = 1.081 \pm 0.015$ [11], with $\chi^2 = 5.2$ for 3 degrees of freedom. Assuming isospin symmetry, we combine the B^0 and B^+ channels and express the results as the B^0 branching fraction in the last row of Table I. The overall χ^2 is 10.2 for 9 degrees of freedom.

We extract $|V_{ub}|$ from the partial branching fractions $\Delta\mathcal{B}$ using $|V_{ub}| = \sqrt{\Delta\mathcal{B}/(\tau_{B^0}\Delta\zeta)}$, where $\tau_{B^0} = (1.536 \pm 0.014)$ ps [11] is the B^0 lifetime and $\Delta\zeta = \Delta\Gamma/|V_{ub}|^2$ is the normalized partial decay rate predicted by the form-factor calculations. We use the light-cone sum rules calculation [5] for $q^2 < 16$ GeV² and the lattice QCD calculations [6, 7, 8] for $q^2 > 16$ GeV². The results are shown in Table II.

In conclusion, we have measured the $B \rightarrow \pi\ell\nu$ branching fraction as a function of q^2 using tagged B meson samples, and have extracted $|V_{ub}|$. The measured total branching fraction, $\mathcal{B}(B^0 \rightarrow \pi^-\ell^+\nu) = (1.33 \pm 0.17_{\text{stat}} \pm 0.11_{\text{syst}}) \times 10^{-4}$, has the smallest systematic uncertainty among the existing measurements [2, 3, 4] thanks to the superior signal purity, and the overall precision is comparable to the best. Using theoretical calculations of the form factor, we obtain values of $|V_{ub}|$ ranging between 3.2×10^{-3} and 4.5×10^{-3} . As an example, the recently published unquenched lattice QCD calculation [6] gives $|V_{ub}| = (4.5 \pm 0.5_{\text{stat}} \pm 0.3_{\text{syst}}^{+0.7}_{-0.5\text{FF}}) \times 10^{-3}$. Improvement will be possible with additional data combined with more precise form-factor calculations.

We are grateful for the excellent luminosity and machine conditions provided by our PEP-II colleagues, and for the substantial dedicated effort from the computing organizations that support *BABAR*. The collaborating institutions wish to thank SLAC for its support and kind hospitality. This work is supported by DOE and NSF (USA), NSERC (Canada), IHEP (China), CEA and CNRS-IN2P3 (France), BMBF and DFG (Germany), INFN (Italy), FOM (The Netherlands), NFR (Norway), MIST (Russia), MEC (Spain), and PPARC (United Kingdom). Individuals have received support from the Marie Curie EIF (European Union) and the A. P. Sloan Foundation.

* Also at Laboratoire de Physique Corpusculaire, Clermont-Ferrand, France

† Also with Università di Perugia, Dipartimento di Fisica, Perugia, Italy

‡ Also with Università della Basilicata, Potenza, Italy

- [1] M. Kobayahi and T. Maskawa, *Prog. Theor. Phys.* **49**, 652 (1973).
[2] S. B. Athar *et al.* (CLEO Collaboration), *Phys. Rev.* **D68**, 072003 (2003).
[3] B. Aubert *et al.* (*BABAR* Collaboration), *Phys. Rev.* **D72**, 051102 (2005).
[4] T. Hokuue *et al.* (Belle Collaboration), hep-ex/0604024.
[5] P. Ball and R. Zwicky, *Phys. Rev.* **D71**, 014015 (2005).
[6] E. Gulez *et al.* (HPQCD Collaboration), *Phys. Rev.* **D73**, 074502 (2006).
[7] M. Okamoto *et al.*, hep-lat/0409116.
[8] A. Abada *et al.*, *Nucl. Phys.* **B619**, 565 (2001).
[9] B. Aubert *et al.* (*BABAR* Collaboration), *Nucl. Inst. & Meth.* **A479**, 1 (2002).
[10] Charge conjugate states are implied throughout this Letter.
[11] S. Eidelman *et al.* (Particle Data Group), *Phys. Lett.* **B592**, 1 (2004).
[12] See EPAPS Document No. E-PRLTAO-97-050647 for two tables containing (i) the systematic errors of the measured partial branching fractions ($B \rightarrow \pi\ell\nu$) and (ii) the error matrices. For more information on EPAPS, see <http://www.aip.org/pubserver/epaps.html>.

Electronic Physics Auxiliary Publication Service (EPAPS)

This is an EPAPS attachment to B. Aubert *et al.* (BABAR Collaboration), Phys. Rev. Lett. **97**, 211801 (2006) [arXiv:hep-ex/0607089]. For more information on EPAPS, see <http://www.aip.org/pubservs/epaps.html>.

TABLE I: Fractional systematic errors (in %) of the measured partial branching fractions. The q^2 bins are defined as 1: $q^2 < 8 \text{ GeV}^2$, 2: $8 < q^2 < 16 \text{ GeV}^2$, and 3: $q^2 > 16 \text{ GeV}^2$. The + and \times symbols indicate if the error is additive (+) or multiplicative (\times).

	B_{tag} bin	B^0 semilep.			B^+ semilep.			B^0 hadronic			B^+ hadronic		
		1	2	3	1	2	3	1	2	3	1	2	3
$B \rightarrow \pi \ell \nu$ form factor	\times	1.0	0.5	1.1	0.9	0.5	4.5	0.3	0.2	0.1	0.3	0.2	2.2
$B \rightarrow X_c \ell \nu$ background	+	1.9	2.9	3.8	2.0	3.5	7.7	0.2	0.2	0.2	2.6	2.6	2.6
$B \rightarrow X_u \ell \nu$ background	+	0.8	1.7	6.9	1.2	1.7	12.1	4.2	4.2	4.2	1.7	1.7	1.7
$\mathcal{B}(B \rightarrow X \ell \nu)$	\times	not applicable						2.6	2.6	2.6	2.6	2.6	2.6
$\mathcal{B}(\Upsilon(4S) \rightarrow B^0 \bar{B}^0)$	\times	1.6	1.6	1.6	1.6	1.6	1.6	not applicable					
Final-state radiation	\times	1.2	1.2	1.2	1.2	1.2	1.2	1.2	1.2	1.2	1.2	1.2	1.2
B_{tag} efficiency	\times	7.3	7.3	7.3	4.3	2.5	12.9	0.7	0.7	0.7	1.4	1.4	1.4
q^2 resolution	\times	1.6	1.3	1.2	1.2	4.5	18.0	negligible					
Fit method	+	1.4	2.1	5.7	4.8	6.2	32.8	5.7	5.7	5.7	2.7	2.7	2.7
Lepton identification	\times	1.6	1.9	1.9	2.5	2.5	2.5	2.5	2.5	2.5	2.5	2.5	2.5
Charged track reconstruction	\times	1.6	1.6	1.6	0.8	0.8	0.8	1.1	1.1	1.1	1.4	1.4	1.4
Neutral energy reconstruction	\times	negligible			3.2	3.0	6.3	1.2	1.2	1.2	3.7	3.7	3.7
Number of $B\bar{B}$ events	\times	1.1	1.1	1.1	1.1	1.1	1.1	not applicable					
MC statistics	\times	5.2	5.1	4.6	4.7	4.2	6.8	18.3	11.8	17.6	19.8	14.7	23.0
Total		10.0	10.4	13.6	9.7	10.9	43.5	20.1	14.4	19.4	21.0	16.3	24.1

TABLE II: Values and errors (in unit of 10^{-4}) of the combined partial branching fractions. The errors are separated into statistical, multiplicative systematic, and non-multiplicative systematic components, and the covariance matrices for the systematic components are given. The q^2 bins are defined as 1: $q^2 < 8 \text{ GeV}^2$, 2: $8 < q^2 < 16 \text{ GeV}^2$, and 3: $q^2 > 16 \text{ GeV}^2$.

	bin	1	2	3
Value		0.355	0.518	0.457
Statistical error		0.086	0.097	0.104
Multiplicative systematic error		0.028	0.038	0.052
Covariance	1	1.000	0.593	0.471
	2	0.593	1.000	0.504
	3	0.471	0.504	1.000
Non-multiplicative systematic error		0.008	0.017	0.021
Covariance	1	1.000	0.986	0.791
	2	0.986	1.000	0.881
	3	0.791	0.881	1.000